NASA Contractor Report 198392

Modeling of Bulk Evaporation and Condensation

S. Anghaie and Z. Ding
University of Florida
Gainesville, Florida

April 1996

Prepared for
Lewis Research Center
Under Contract NAS3–26314

National Aeronautics and
Space Administration

TABLE OF CONTENTS

ABSTRACT

This report describes the modeling and mathematical formulation of the bulk evaporation and condensation involved in liquid-vapor phase change processes. An internal energy formulation, for these phase change processes that occur under the constraint of constant volume, was studied. Compared to the enthalpy formulation, the internal energy formulation has a more concise and compact form. The velocity and time scales of the interface movement were obtained through scaling analysis and verified by performing detailed numerical experiments. The convection effect induced by the density change was analyzed and found to be negligible compared to the conduction effect. Two iterative methods for updating the value of the vapor phase fraction, the energy based (E-based) and temperature based (T-based) methods, were investigated. Numerical experiments revealed that for the evaporation and condensation problems the E-based method is superior to the T-based method in terms of computational efficiency. The internal energy formulation and the E-based method were used to compute the bulk evaporation and condensation processes under different conditions. The evolution of the phase change processes was investigated. This work provided a basis for the modeling of thermal performance of multi-phase nuclear fuel elements under variable gravity conditions, in which the buoyancy convection due to gravity effects and internal heating are involved.

NOMENCLATURE

A, C, D	constants
E	internal energy [J]
H	enthalpy [J]
Q	heat quantity [J]
T	temperature [K]
V	volume [m^3]
U	velocity [m/s]
W	work [J]
X, R	dimensionless coordinates
c_v, c_p	specific heat at constant volume and constant pressure [J/kg/K]
e	specific internal energy [J/kg]
h	specific enthalpy [J/kg]
f	vapor phase fraction
l	length scale [m]
p	pressure [bar]
t	time [s]
x, r	cylindrical coordinates [m]

Greek symbols

α	thermal diffusivity [m^2/s], or thermal diffusivity ratio
ε	phase-change temperature interval
κ	thermal conductivity [W/K/m], or its ratio

O	order of magnitude
θ	dimensionless temperature
ρ	density [kg/m^3], or its ratio
τ	dimensionless time

Subscripts

f	interface position, mixed phase
i	interface
l	liquid phase
r	characteristic scale
s, sat	saturation point
v, vap	vapor phase

Superscripts

k	iteration level
n	time level

CHAPTER 1 INTRODUCTION

In recent years, phase change processes such as melting and solidification, boiling and condensation have attracted increasing interest in their development and applications. Among these activities, numerical modeling and simulation of the phase change processes have been the focus of many investigators. The purpose of this work is to develop a consistent numerical method for the computation of the bulk evaporation and condensation processes involved in a specific class of liquid-vapor phase change problems under constant volume and no buoyancy conditions. The need for the development of such models has been promoted by a recent investigation aiming to establish the feasibility of using an encapsulated two-phase nuclear fuel for high temperature space power and propulsion applications.

Numerical modeling of heat transfer problems involving phase change has been discussed by a large number of investigators [1-14]. Shyy [11] presented a comprehensive discussion of the various computational elements important for the prediction of complex fluid flows and interfacial transport. Most of the noted investigators have approached the solid-liquid phase change problems, such as those involved in melting and solidification processes. There has also been an ongoing interest in the investigation of liquid-vapor phase change problems, such as evaporation and condensation. More attempts have been made to numerically model and simulate condensation phenomena. In particular, a number of investigators have developed numerical models for flow condensation problems [15 - 18]. Most of this numerical modeling has focused on parabolic flow condensation problems where the forced convection plays a dominant role. In this type of condensation problem, the vapor pressure, saturation temperature and latent heat have

been treated as constant properties. In the present study, the saturation temperature, and pressure are modeled as dependable variables. In a more recent work, Jang et al. [19] have modeled a heat pipe start-up from the frozen state by using the a system of simplified one dimensional equations. Shyy et al. [20] have successfully developed a computational method for predicting the two-phase transient flow and heat transfer characteristics within a constant pressure reservoir of a capillary-pumped-loop and investigated the phase change of liquid and vapor, under various conditions. The present approach has expanded the mathematical modeling of the phase change problems by including the pressure as a dependent variable and using the internal energy formulation.

The numerical models for the phase change problems can be divided into two groups, based on the choice of dependent variables. In the first group, temperature is the sole dependent variable, and energy equations are written separately for the solid and liquid phases. In the second group, enthalpy is used as the main dependent variable along with the temperature. This formulation which is widely used by many investigators is known as the enthalpy method. In the enthalpy model, the phasic interface is eliminated from the formulation and the problem is made equivalent to a nonlinear heat conduction problem without phase change. Shamsunder and Sparrow [3] and Shyy [11] summarized these features and demonstrated the usefulness of the enthalpy formulation. The enthalpy formulation has been employed in many investigations [3, 9, 10, 11, 20].

This report presents a discussion of the bulk evaporation and condensation processes taking place in a constant volume container without vapor bubble or liquid droplet generation and boiling. This problem can be depicted with the case presented in Fig.1. A rigid, cylindrical container is partially filled with vapor and liquid. Initially, the vapor and liquid are kept saturated at a certain pressure and uniform temperature. Well selected boundary conditions on the walls are imposed to activate the pure bulk evaporation or condensation, and also to avoid the buoyancy

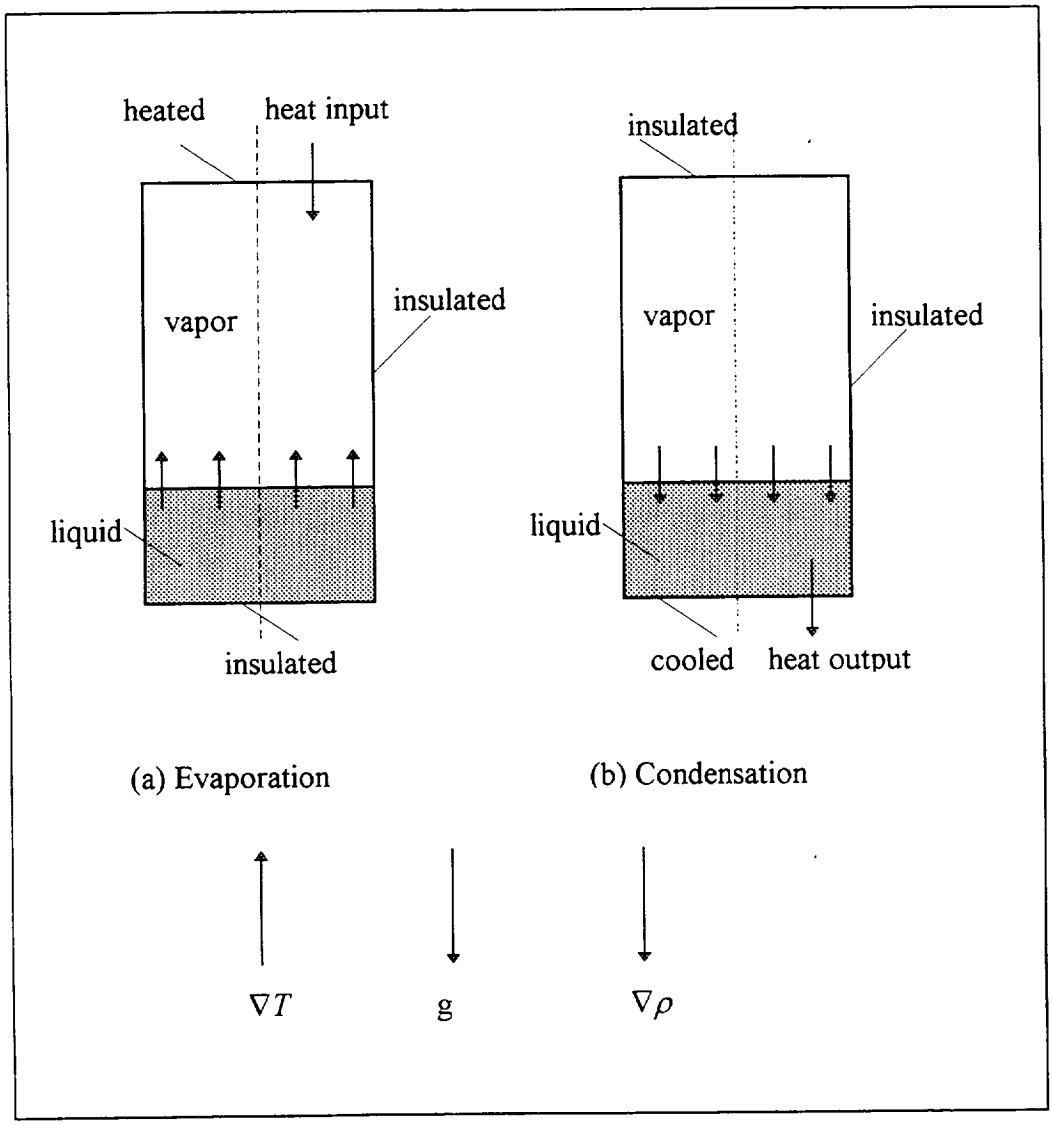

Figure 1.1 Schematic of the bulk evaporation and condensation

effect and bubble generation. While keeping the side wall insulated, only heating the top wall or cooling the bottom wall induces pure evaporation or condensation, respectively. The volumetric expansion or contraction due to the density change between two phases induces convection in the vapor phase. The scaling analysis conducted in this work indicates that this convection effect is quite week and negligible. It can be reasonably assumed that the phase change processes are

driven entirely by the conduction and the release or absorption of latent heat at the phase change interface. Similar situations are also possible for the multi-dimentional phase-change problems in zero gravity condition.

No expansion work is involved in this constant volume phase change process. In the absence of mechanical work, the first law of thermodynamics indicates that the heat exchange between the system and the ambient equals the change of the internal energy of the system. The released or absorbed latent heat associated with the phase-change is equal to the change of internal energy. Based on the physical conditions of this system, a compact internal energy formulation of the energy equation is proposed. This formulation, similar to the enthalpy formulation, is a single region formulation, where one set of governing equations can describe both phases.

CHAPTER 2 FORMULATION

The first law of thermodynamics, for any thermodynamic system, is

$$\delta Q = dE + \delta W = dH - (pdV + Vdp) + \delta W \tag{2.1}$$

where E is the internal energy, H is enthalpy, Q is the heat input, W is the work output, p and V are the pressure and volume of the system, respectively. For the phase change process involved in the rigid and enclosed container with constant volume, there is no mechanical work. Therefore the first law for this closed and rigid system reduces to

$$\delta Q = dE = dH - Vdp \tag{2.2}$$

which indicates that the heat exchange between the system and the ambient causes the internal energy, the enthalpy and pressure of the system to change. Therefore the released or absorbed latent heat associated with the phase change induces the changes of internal energy, enthalpy and pressure. The quantity of the heat exchange is equal to the internal energy change, but not equal to the enthalpy change. The conventional enthalpy formulation of the energy equation, commonly used for the phase change between solid and liquid, should include a transient pressure term for this phase change between liquid and vapor. The weak form of the energy equation based on enthalpy formulation is

$$\rho \frac{Dh}{Dt} = \frac{Dp}{Dt} + \nabla \cdot (\kappa \nabla T) \tag{2.3}$$

This formulation including the transient pressure term introduces additional complexity and does not seem to be the best choice for this problem. A more attractive alternative, the internal energy based formulation for the energy equation which does not include the pressure term, is proposed and developed in this work. Similar to the enthalpy formulation used for melting

and solidification problems, the internal energy formulation does not require to explicitly track the interface position.

The weak form of the energy equation with internal energy as the primary variable can be expressed as follows:

$$\rho \frac{De}{Dt} = \nabla \cdot (\kappa \nabla T) \tag{2.4}$$

where the internal energy e may be expressed, in the form of a summation of sensible heat and latent heat, for the liquid, vapor and mixed phases as:

$$\begin{aligned} e &= c_{v,l} T && f = 0 \\ e &= c_{v,l} T_{sat} + f\Delta e && 0 < f < \\ e &= c_{v,l} T_{sat} + \Delta e + c_{v,v} (T - T_{sat}) && f = 1 \end{aligned} \tag{2.5}$$

where T_{sat} is the saturation temperature, Δe is the internal energy difference between saturated vapor and saturated liquid (latent heat), and the constant volume specific heat c_v's are functions of temperature provided by Reynolds [21]. The vapor phase fraction f is zero in the region filled with liquid phase and unity in the region occupied by vapor phase. The vapor phase fraction lies between zero and unity when the control volume is undergoing phase change.

Substituting Eq.(1.5) into the governing Eq.(1.4) yields

$$\begin{aligned} \rho_l \frac{D}{Dt}(c_{v,l} T) &= \nabla \cdot (\kappa_l \nabla T) && f = 0 \\ \rho_f \frac{D}{Dt}(c_{v,f} T) &= \nabla \cdot (\kappa_f \nabla T) - \rho_f \Delta e \frac{Df}{Dt} && 0 < f < 1 \\ \rho_v \frac{D}{Dt}(c_{v,v} T) &= \nabla \cdot (\kappa_v \nabla T) && f = 1 \end{aligned} \tag{2.6}$$

where the latent heat now appears as a source term. The form of this internal energy based equation is identical to that of the enthalpy based equation, except the pressure term appearing in

the later one. Just like the enthalpy formulation, this internal energy formulation is also a single region formulation, where one set of governing equations can describe both phases. A major advantage of the internal energy formulation is that it is not necessary to split the domain into separate subdomains consisting of different phases. A fixed grid can be employed to facilitate the computations.

Both enthalpy formulation and internal energy formulation are implemented and examined. The vapor phase fraction, f, may be defined in two different ways, which can lead to different update methods.

Some additional closure relations are required for the multiphase condition in the container. Property variations are based on a simplified searching routine. The different phases are differentiated based on the local temperature or internal energy at each nodal point, within the frame work of the temperature based or internal energy based update method. Using temperature based update, the liquid or the vapor phase is identified by the local temperature, wherever the temperature at any point is lower than the saturated liquid temperature or higher than the saturated vapor temperature, that point is located in the liquid or vapor region, respectively. Similarly, if the internal energy based update is used, the liquid or the vapor phase is identified by the local internal energy. Either case allows the vapor phase fraction in a computational cell to be calculated.

Using the Clausius-Clapeyron equation, the saturation temperature as a function of the system pressure is calculated:

$$T_{sat} = \frac{C}{D - \ln p_{sat}} \tag{2.7}$$

where C and D are constants.

The saturation pressure, or the vapor pressure, can be obtained from the approximate equation of state for an ideal gas, and the mass conservation in which the bulk vapor density and temperature are used:

$$p_{sat} = p_{vap} = \frac{m_v}{V_{vap}} R T_{b,vap}, \qquad m_{total} = m_v + m_l = Constant \tag{2.8}$$

where R is the gas constant for vapor phase. Eqs.(2.7) and (2.8), have been proposed and used as the basis for the model developed by the authors, Ding and Anghaie [22, 23].

CHAPTER 3 ANALYSIS AND DISCUSSION

To simplify and generalize the formulation for the bulk evaporation and condensation processes, these governing equations and closure relationships should be normalized. Scaling and analysis of order of magnitude are conducted to develop simplifying assumptions that lead to a concise and efficient solution procedure for the governing equations. For the different phases of any material, the thermodynamic and transport properties are quite different, and they may be in the same order or may have a difference of several orders of magnitude. For the same phase, some properties are independent or slightly dependent on temperature or pressure, but others may be strongly dependent. The following relations are found about the orders and variations of these properties, for liquid and vapor phases far from the thermodynamic critical point, within a moderate phase-change range.

$$\begin{aligned}
&c_{v,l} \cong constant, && c_{v,v} \cong constant, && \frac{c_{v,l}}{c_{v,v}} \sim O(1), \\
&\kappa_l \cong constant, && \kappa_v \cong constant, && \kappa = \frac{\kappa_l}{\kappa_v} \sim O(10) - O(10^2), \\
&\rho_l \cong constant, && \rho_v \neq constant, && \rho = \frac{\rho_l}{\rho_v} \sim O(10^2) - O(10^3), \\
&\alpha_l \cong constant, && \alpha_v \neq constant, && \alpha = \frac{\alpha_l}{\alpha_v} \sim O(10^{-1})
\end{aligned} \tag{3.1}$$

where ' $\cong$ constant ' means that the variation is within one order of magnitude, and ' O ' represents the order of magnitude.

Therefore all the properties, except the vapor density and vapor thermal diffusivity, can be assumed constant. The liquid specific heat and vapor specific heat are assumed equal. In the following analysis and computation, these values of the ratios such as $\kappa = \frac{\kappa_l}{\kappa_v} = 10, . \rho_0 = \frac{\rho_l}{\rho_{v,0}} = 10^2, . \alpha_0 = \frac{\alpha_l}{\alpha_{v,0}} = 10^{-1}$ are used, where the subscript 0 denotes a reference state.

As discussed in some literature [1, 24], due to the density difference between two different phases, the volumetric expansion effect induces the convection in the phase of lower

density. Let Ui denote the speed for the motion of the interface and Uv for the motion of the vapor phase resulting from the density change. The mass conservation at the interface should be satisfied as follows

$$\rho_l U_i = \rho_v (U_i - U_v) \tag{3.2}$$

The energy-balance equation at the interface is

$$\kappa_l \frac{\partial T_l}{\partial x} - \kappa_v \frac{\partial T_v}{\partial x} + \rho_v e_v U_v = (\rho_v e_v - \rho_l e_l) U_i \tag{3.3}$$

where e_v and e_l denote the internal energies for the saturated vapor and liquid phases, respectively.

Eliminating U_v from Eq.(3.3) via Eq.(3.2) yields

$$q_{i,v} - q_{i,l} = \kappa_l \frac{\partial T_l}{\partial x} - \kappa_v \frac{\partial T_v}{\partial x} = \rho_l \Delta e U_i \tag{3.4}$$

where $q_{i,v}$ and $q_{i,l}$ represents the heat flux in the interface at the vapor side and liquid side, respectively.

Eq.(3.4) can be rearranged as

$$U_i = \frac{1}{\rho_l \Delta e}(\kappa_l \frac{\partial T_l}{\partial x} - \kappa_v \frac{\partial T_v}{\partial x}) = St(\frac{\alpha_l}{l_t}\frac{\partial \theta_l}{\partial X} - \frac{\alpha_v}{l_t}\frac{1}{\rho}\frac{\partial \theta_v}{\partial X}) \tag{3.5}$$

where l_t is the thermal diffusion length scale which is the length of the container, $St=c_v T_0/\Delta\varepsilon$, $\theta=T/T_0$, $X=x/l_t$, $\rho=\rho_l/\rho_v$. There are two possible velocity scales at the interface, i.e., $U_1=St(\alpha_l/l_l)$, $U_2=St(\alpha_v/l_l)/\rho$, and their ratio is $\frac{U_1}{U_2} = \frac{\alpha_l}{\alpha_v}\frac{\rho_l}{\rho_v} = \alpha \cdot \rho \sim O(10^{-1}) \cdot O(10^2) \sim O(10)$, $U_1 > U_2$.

Therefore it is reasonable to assume that the lower velocity scale U_2 controls the movement of the interface.

Eq.(3.5) can also be expressed as

$$U_i = U_1 \frac{\partial \theta_l}{\partial X} - U_2 \frac{\partial \theta_v}{\partial X} \tag{3.6}$$

The velocity, $U_2=St(\alpha_v/l_t)/\rho$, includes the density change effect which actually reveals the constraints of energy balance and mass conservation at the interface, and the volumetric expansion or contraction during evaporation or condensation, respectively. It is lower than the pure thermal diffusion velocity in liquid, α_l/l_t and that in vapor α_v/l_t. Thus U_2 is to be chosen as the characteristic velocity scale where the density change effect, as well as the S_t number, appears explicitly. The dimensionless velocity of the interface movement is

$$\overline{U}_i = \frac{U_i}{U_2} = \kappa \frac{\partial \theta_l}{\partial X} - \frac{\partial \theta_v}{\partial X} \tag{3.7}$$

For the case of evaporation, for example, heat is supplied to the system from the top wall which is the boundary for the vapor phase. If the appropriate amount of heat flux is provided to ensure $\frac{\partial \theta_v}{\partial X} \sim O(1)$, it is found that $\overline{U}_i \sim O(1)$, thus $Ui \sim Ur = S_t(\alpha_v / l_t)/\rho$. Numerical results which will be shown in the next chapter are compatible with this expression.

The characteristic time scale is

$$t_r = \frac{l_t}{U_r} = \frac{l_t^2}{\alpha_v} \frac{\rho}{S_t} \tag{3.8}$$

Obviously this time scale is larger than those of thermal diffusion in vapor and liquid phases, that is, $\frac{l_t^2}{\alpha_v}\rho > \frac{l_t^2}{\alpha_l} > \frac{l_t^2}{\alpha_v}$, which implies that the motion of the interface controls the rate of this heat transfer process. From the above analysis, it can be conclude that the motion of the interface is affected by the density difference between liquid and vapor phases, thus its velocity is

very low. During the evaporation process with constant system volume, density change increases the vapor pressure and the saturation temperature, which in turn suppresses the evaporation.

From Eqs.(3.2) and (3.7), the velocity of vapor convection induced by the density change is $Uv = (1-\rho)Ui \sim \frac{1-\rho}{\rho}\frac{\alpha_v}{l_t}S_t$, and since $\rho >> 1$, $U_v \sim (\alpha_v/l_t)St$, which is still very low. Therefore the Reynolds number and Peclet number for the convection are $Re = U_v l_v / \nu_v = (l_v/l_t)(St/Pr)$, $Pe = (l_v/l_t)\, St.$, where l_v is the vapor motion length scale. Since the velocity of the vapor convection is very low, and the convection just occurs near the interface, the vapor convection length scale will be very small compared to the thermal diffusion length scale, say, $l_v/l_t < O(1)$. For most vapors, $Pr \sim O(1)$, and if moderate St is considered, i.e., $St \sim O(1)$, then $Re < O(1)$, and $Pe < O(1)$. For the problems in which Re and Pe are less than the order of unity, the convection effect is weaker than the molecular movement effect and hence insignificant. Therefore the thermal diffusion, i.e., the heat conduction, dominates the heat transfer process and the convection effect induced by the density change is negligible.

On the other hand, it can be found that the convection effect caused by the density change during phase change is much less significant than the convection induced by buoyancy effect when encountered. The characteristic velocity of the natural convection is $Ur = (Gr)^{1/2}\, \nu/L$ where Gr is the Grashof number, the corresponding Reynolds number $Re = UrL/\nu = (Gr)^{1/2}$. If $Gr = 10^4 \sim 10^6$, then $Re = 10^2 \sim 10^3$, which is stronger than the density change effect.

From this analysis, the convection effect can be reasonably neglected and the bulk evaporation and condensation processes can be assumed entirely driven by heat conduction. The governing equations (2.6) can be reduced to the heat conduction-driven phase-change problems:

$$\rho_l \frac{\partial}{\partial t}(c_{v,l} T) = \nabla \cdot (\kappa_l \nabla T) \qquad f = 0$$

$$\rho_f \frac{\partial}{\partial t}(c_{v,f} T) = \nabla \cdot (\kappa_f \nabla T) - \rho_f \Delta e \frac{\partial f}{\partial t} \qquad 0 < f < 1 \qquad (3.9)$$

$$\rho_v \frac{\partial}{\partial t}(c_{v,v} T) = \nabla \cdot (\kappa_v \nabla T) \qquad f = 1$$

Eq.(3.9) can also be written in terms of dimensionless parameters as:

$$\frac{S_t}{\rho}\frac{\partial \theta}{\partial \tau} = \alpha \nabla^2 \theta \qquad f = 0$$

$$\frac{S_t}{\rho}\frac{\partial \theta}{\partial \tau} = \alpha \nabla^2 \theta - \frac{1}{\rho}\frac{\partial f}{\partial \tau} \qquad 0 < f < 1 \qquad (3.10)$$

$$\frac{S_t}{\rho}\frac{\partial \theta}{\partial \tau} = \nabla^2 \theta \qquad f = 1$$

Here S_t is the Stefan number defined as $c_v T_{s,0}/\Delta\varepsilon$, where $T_{s,0}$ is the initial saturation temperature. $T_{s,0}$ and the length of the container are chosen as the characteristic temperature scale and length scale, respectively. The characteristic time scale is shown in Eq.(16). The relationships presented in Eqs. (2.7) and (2.8) are nondimensionalized as

$$\theta_S = \frac{A}{A - \ln(\bar{p}_S)}, \qquad \bar{p}_S = \bar{\rho}_V \theta \qquad (3.11)$$

where $\bar{p}_s$ and $\bar{\rho}_v$ are dimensionless saturation pressure and vapor density, respectively.

CHAPTER 4 VAPOR PHASE FRACTION UPDATE

To solve the physical model described by Eq.(3.10), a closure relationship between the vapor phase fraction f and the temperature θ or the internal energy e should be formulated. For a pure substance undergoing evaporation or condensation, the total internal energy is a discontinuous function of the temperature:

$$\begin{aligned} \bar{e} &= \frac{e}{\Delta e} = S_t \cdot \theta && \theta < \theta_{sat} \\ \bar{e} &= \frac{e}{\Delta e} = S_t \cdot \theta + 1 && \theta > \theta_{sat} \end{aligned} \tag{4.1}$$

where θ_{sat} is the saturation temperature. However, from a computational viewpoint, discontinuities are difficult to track and it is often necessary to smear the phase change over a small temperature range to attain numerical stability. Thus we can have

$$\begin{aligned} \bar{e} &= S_t \cdot \theta && \theta < \theta_l \\ \bar{e} &= S_t \cdot \theta_l + (\theta - \theta_l)/(\theta_v - \theta_l) && \theta_l < \theta < \theta_v \\ \bar{e} &= S_t \cdot \theta + 1 && \theta_v < \theta \end{aligned} \tag{4.2}$$

where $\theta_l = \theta_{sat} - \varepsilon$, $\theta_v = \theta_{sat} + \varepsilon$, and ε is the phase change interval. As a result, the discontinuity is replaced by a small window, 2ε, over which the phase change occurs. For a pure substance, this window is a purely numerical artifact and must be chosen as small as possible in order to accurately model the physical system. Substitution of Eq.(4.2) into the normalized form of Eq.(2.5) yields

$$f = \frac{\theta - \theta_l}{\theta_v - \theta_l} = \frac{\theta - \theta_l}{2\varepsilon} \tag{4.3}$$

which is used to iteratively update the phase fraction from the computed temperature field. This technique has been successfully used by Shyy et al. [10, 11, 20] and was referred to as the T-based update method. This technique has proven to be very effective for achieving convergence. An alternative formulation to the T-based update method is to express the phase fraction as a function of the total enthalpy rather than the temperature. This update is referred to as the H-based update method. More information about this method can be found in Ref. [10, 11].

A third formulation expressing the vapor phase fraction as a function of the total internal energy, rather than the temperature or enthalpy, is developed in this work. According to the classical thermodynamic definition, the relationship between the vapor phase fraction and the internal energy is

$$f = \bar{e} - \bar{e}_l \tag{4.4}$$

This is used for the iterative update of the vapor phase fraction. This update procedure is referred to as the E-based update method and is similar to the isothermal case discussed by Voller and Swaminathan [2]. In particular, it is noted that $\varepsilon=0$ is allowable in this formulation, thereby allowing for modeling phase change of a pure substance with higher accuracy. This is the most important advantage of the E-based method compared to the T-based method where a significant effort must be made to determine the phase change temperature interval ε. For the phase change problems involving complex interface geometry, the normal temperature gradient varies with the positions along the interface. The determination of the phase change intervals for such problems is a tedious task. The E-based method does not need to use a phase change window and can be

conveniently used for all kinds of phase change problems including the ones with complicated geometry. Another advantage of the E-based method is the fact that if the latent heat is large relative to the sensible internal energy, the vapor phase fraction varies slowly with respect to the total internal energy. This enhances the stability of the update procedure. For the liquid-vapor phase change occurring far away from its critical point, the latent heat is relatively large and the application of the E-based update method even for simple geometry is recommended. In the present work, the T-based and E-based methods are examined in details from the viewpoint of accuracy and computational efficiency.

A straight-forward implementation of the T-based method to discretize Eq. (3.10) for each computational cell yields:

$$a_P\theta_P{}^k = \Sigma a_{nb}\theta_{nb}{}^k + b^k - \frac{\Delta V}{\rho\Delta\tau}[f_P{}^{k-1} - f_P{}^{n-1}] \tag{4.5}$$

where the subscript P represents the nodal point of the control volume to be solved, and nb represents the neiboring nodal points. This equation is solved according to the T-based update procedure given in Eq.(4.3). As reported by Shyy et al.[9, 10] and Prakash et al. [5], for Stefan number less than unity (large values of latent heat), this form of the iterative update is prone to numerical instability in the form of oscillations. For moderate values of Stefan numbers, the use of an under-relaxation approach for the calculation of the source term facilitates the solution process. The main cause of the oscillatory, non-convergent behavior is the extreme sensitivity of the vapor fraction to small changes in temperature which leads to a large negative feedback effect through the source term.

Substituting Eq.(22) into the discrete form of the conservation law and moving the resulting coefficients of T_P into the a_P term in Eq.(24), yields a set of stable equations similar to those formulated by Shyy et al. [9]. These equations are:

$$\begin{aligned} a_P\theta_P{}^k &= \Sigma a_{nb}\theta_{nb}{}^k + b^k - \frac{\Delta V}{\rho\Delta\tau}[f_P{}^{n-1} - f_P{}^{k-1}] && \theta_P{}^{k-1} < \theta_l, or\, \theta_P{}^{k-1} > \theta_v \\ [a_P + \frac{\Delta V}{\rho\Delta\tau}\frac{1}{2\varepsilon}]\theta_P{}^k &= \Sigma a_{nb}\theta_{nb}{}^k + b^k + \frac{\Delta V}{\rho\Delta\tau}[\frac{\theta_l}{2\varepsilon} + f_P{}^{n-1}] && \theta_l \le \theta_P{}^{k-1} \le \theta_v \end{aligned} \tag{4.6}$$

where the superscript n indicates the current time step and k indicates the current iterative value. Using this form of the update procedure, the temperature and the vapor phase fraction fields can be computed simultaneously and are therefore coupled at every step of the iterative process. This numerical procedure converges quickly with no loss of accuracy, granted that a proper value of ε is used.

The implementation of the E-based method is relatively straightforward and does not need any pre-conditioning. The internal energy is updated first, with the current values of saturation temperature and latent heat,

$$\bar{e}_P{}^k = S_t\theta_P{}^k + f^{k-1} \quad , \qquad 0 < f^{k-1} < \tag{4.7}$$

Then the vapor phase fraction is updated with the current internal energy,

$$f^k = \bar{e}_P{}^k - \bar{e}_l{}^k \quad , \qquad \bar{e}_l{}^k < \bar{e}_P{}^k < \bar{e}_v{}^k \tag{4.8}$$

where $e_l = St\theta_{sat}$ and $e_v = e_l + \Delta e$.

CHAPTER 5 RESULTS AND DISCUSSION

5.1 Accuracy Issues

A testing case of pure bulk evaporation is selected to examine the accuracy, the computational performances of each formulation with different update methods. A fixed volume container with one fourth volume filled with a saturated liquid is analyzed. The rest of the container's volume is filled with the saturated vapor. The initial temperature of the saturated fluid is 1.0. The top wall is heated and kept at a temperature of 1.5, while the bottom wall is insulated. Such an orientation of heat flow is required to avoid the bubble generation and boiling, while the bulk evaporation is allowed. A mesh of *81x6* non-uniform and fixed grids is adopted for the liquid and vapor within the container. The time step size $\Delta\tau=10^{-4}$ is chosen. The second order central differences are used for all spatial derivative terms and the fully implicit difference is employed for the time marching.

Figs.5.1(a) and (b) show the evolution of the evaporation process. At the time instant of 0.03, about 18% of liquid is vaporized, and the saturation temperature is about 1.38. A little wavy or non-uniform variation can be seen due to the nature of the discretization and the non-uniform release or absorption of the latent heat. A significant part of the latent heat content in a computational cell is absorbed when it starts to undergo evaporation. Thus the interface movement is slowed down when phase change in this cell starts and subsequently speeds up.

The grids are clustered near the liquid-vapor interface, and the finer grids are placed near the interface and covering the range of the interface movement. Different minimum grid sizes, i.e., $\Delta X_{min}=1/100,\ 1/200,\ 1/400$, are selected to examine the solution accuracy and the independence of solution on the grid size. The results with different minimum grid sizes are basically identical, while the finer grid size yields smoother solution. In the following computations, the grid size with $\Delta X_{min}=1/200$ is used.

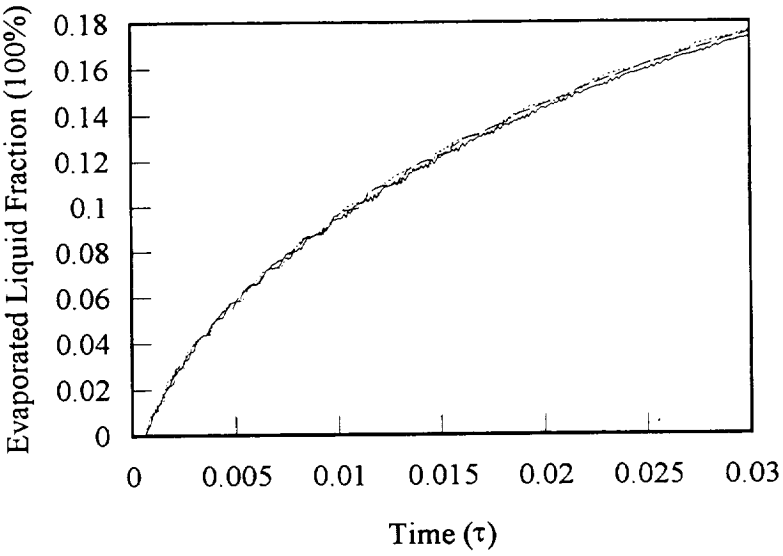

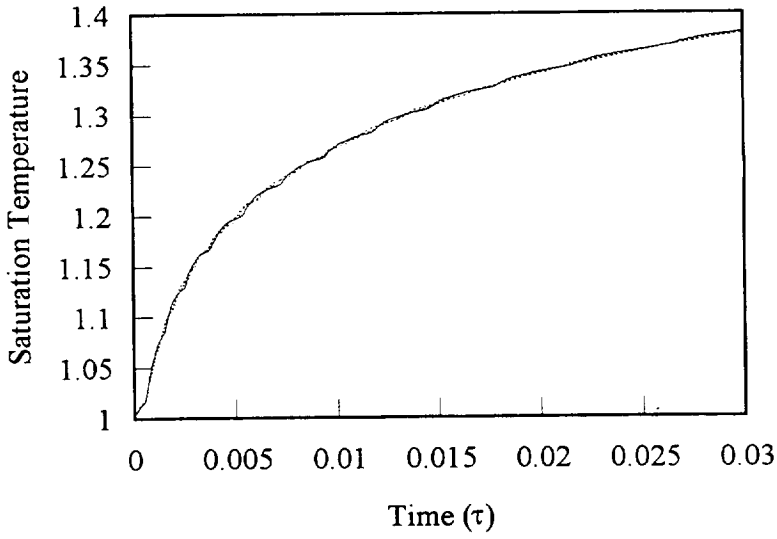

Figure 5.1 Solution features for bulk evaporation (Grids 81x8, ΔX_{min}=1/120, 1/200, 1/400)

5.2 Comparison of H-Formulation and E-Formulation

The same testing case is computed to examine the performances of different formulations, the enthalpy formulation and internal energy formulation. Figs.5.2(a) and (b) show the evaporated liquid fraction and the variation of the saturation temperature during the evaporation process. Fig.5.2(c) shows the efficiency of the computations, that is, the number of iterations required at each time step for the residual to go below 10^{-4}. The enthalpy formulation needs a few more iterations for convergence of the calculation. It can be found that the internal energy formulation and enthalpy formulation yield nearly identical results, with close computational efficiency. It indicates that both of these formulations are proper for this problem and have similar efficiency performance. The only advantage in the internal energy formulation is the more concise form without an explicit pressure term. In the following investigations, only the internal energy formulation is adopted.

5.3 Comparison of E-Based and T-Based Update Methods

The T-based update method and the E-based update method are examined for the same testing case. Figures 5.3(a) and (b) show that the T-based method and E-based method yield nearly identical results. It can be seen that for convergence the E-based method requires about half of the iterations which is needed for the T-based method. Thus the E-based method is computationally more efficient than the T-based method, as shown in Fig.5.3(c). The efficiency performances of these two update methods for the evaporation and condensation problems are different from those for melting and solidification problems where the T-based is better than H-based method as reported [10].

The reason for the improved efficiency of the E-based method is that the phase change temperature window is used for the T-based method, which is not required for the E-based method. When the T-based method is used and the purely artificial phase change window has to be adopted, it is not easy to use the temperature to identify the phase interface since the temperature is always continuous at the interface. For melting and solidification problems, the phase change temperature is usually constant. The saturation temperature, however, changes continuously for evaporation and condensation processes in a constant volume system. This difference causes distinctive computational efficiency performances. For each iteration at every time step, the saturated vapor and liquid temperature as well as the saturation temperature should be updated. Therefore, the T-based method converges more slowly. When the E-based method is used, the internal energy has a sharp jump at the interface, it is easy to use internal energy to identify the phases. As has been mentioned before, the relative large amount of the latent heat will result in a more stable update procedure and faster convergence rate. Furthermore, as discussed in the section of update methods, if the T-based method is used, there will be some difficulty to determine the phase change temperature intervals for the complicated phase change problems where the interface could be of any arbitrary shape. Using the E-based method can completely circumvent the need for a phase change window. Therefore, the E-based method is superior to the T-based method, in terms of computational efficiency and formulation simplicity, and is capable of handling more complicated phase change geometry.

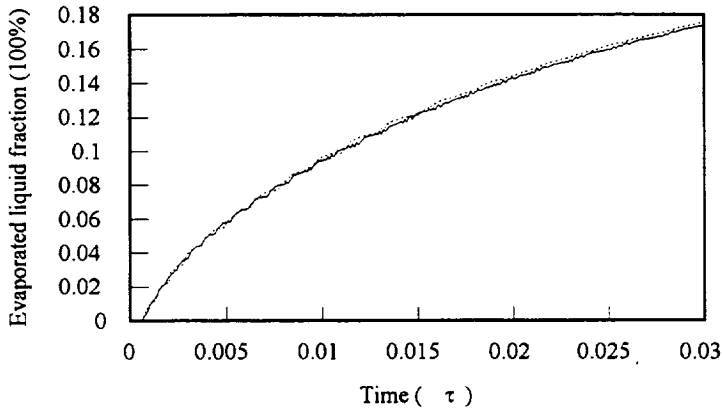

(a) evolution of vaporization

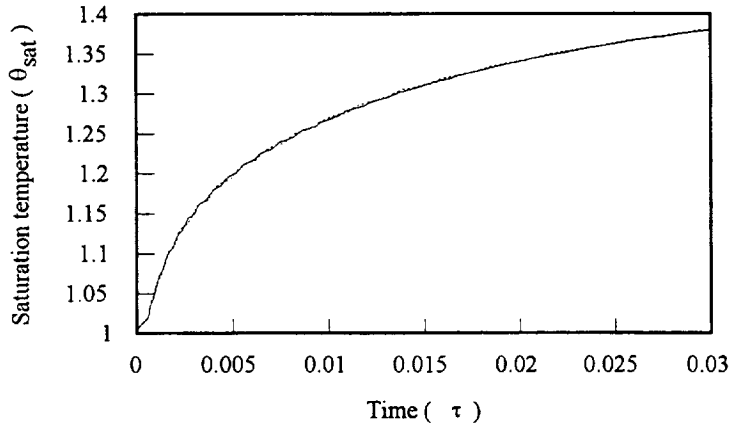

(b) variation of saturation temperature

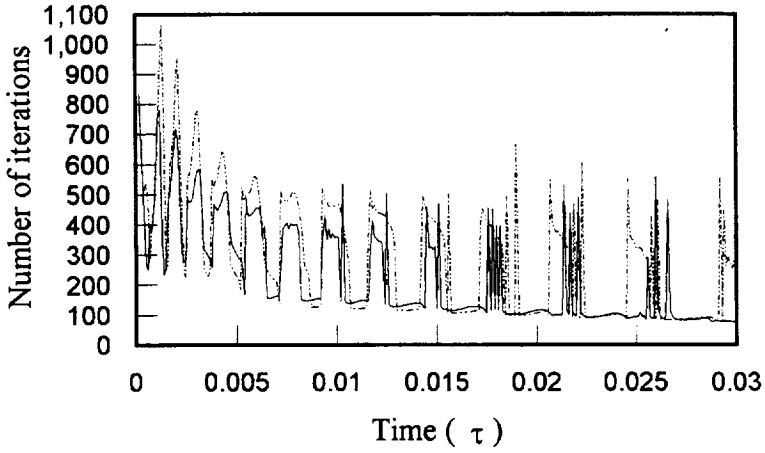

(c) computation efficiency performance

Figure 5.2 Comparison of two formulations for evaporation
The solid line: the internal energy formulation; the dashed line: the enthalpy formulation

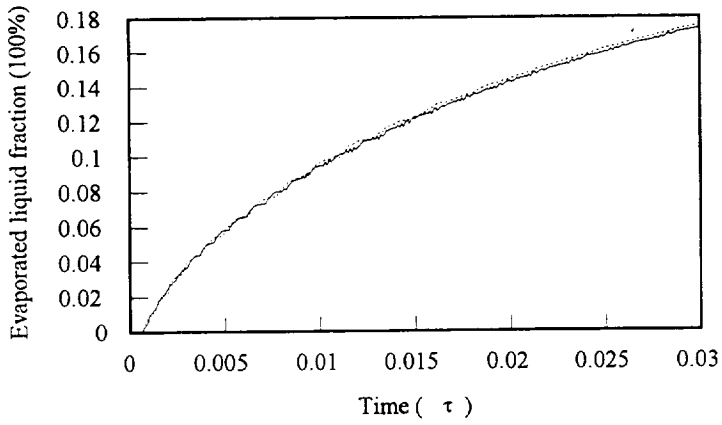

(a) evolution of vaporization

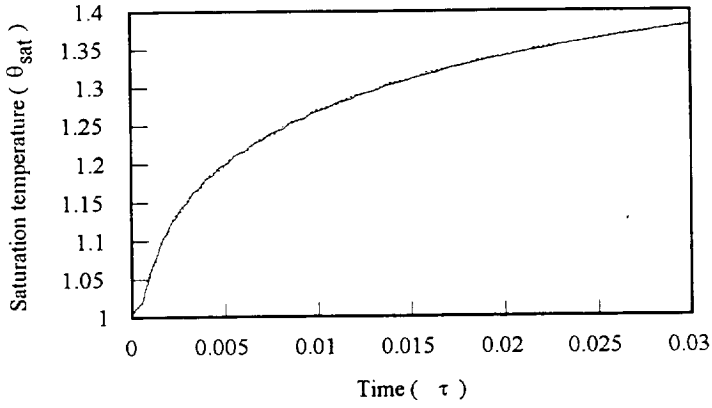

(b) variation of saturation temperature

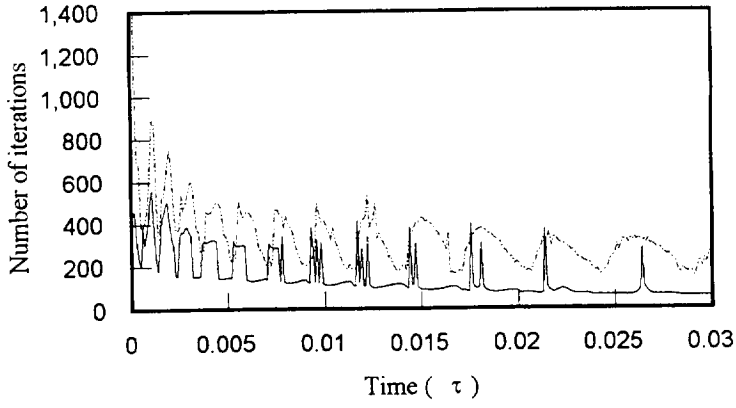

(c) computation efficiency performance

Figure 5.3 Comparison of two update methods for evaporation
The solid line: the E-based method; the dashed line: the T-based method

5.4 Bulk Evaporation, Condensation and the Interface Motion Scale Analysis

In the following work, the internal energy formulation and the E-based update method are used to investigate the bulk evaporation and condensation processes and also to analyze the interface motion scale. With other conditions remaining the same, i.e., the initial temperature, the grid distribution and the time step size, different boundary conditions are imposed at the top and bottom walls. First, the container's top wall is heated with a constant heat flux $q_{tw} = \frac{\partial \theta_v}{\partial X}|_{X=0} = 1.0$, and the bottom wall is insulated. After the time instant of 0.02, the top wall is insulated while the bottom wall is cooled with a constant heat flux $q_{bw} = \kappa \frac{\partial \theta_l}{\partial X}|_{X=1.0} = 10x1.0 = 10$. Correspondingly, the system undergoes an evaporation-condensation process. Fig.5.4(a) shows the variation of the saturation temperature during the transient. The motion of the interface, which is downward and upward during the evaporation and condensation, respectively, is exhibited in Fig.5.4(b). The axial temperature distributions at different time instants during the evaporation process are plotted in Fig.5.4(c), and those of condensation process are plotted in Fig.5.4(d).

The velocity of the interface motion can be calculated from results presented in Fig.5.4(b). During the evaporation and condensation processes, the interface velocity is always constant because only the constant heat flux at either the top wall or bottom wall is provided. During the evaporation process which takes place with a constant heat flux at the top wall, the interface velocity is a constant about 2.5, which is in the order of 1.0. While during the condensation process with a constant heat flux at the bottom wall, the interface velocity still remains constant at the level of about 0.8. This indicates clearly that the nondimensional interface velocity is consistently of the order of 1.0. In other words, it can be concluded that $\overline{U}_i \sim O(1)$, thus $Ui \sim Ur = S_t(\alpha_v / l_t) / \rho$. This analysis verifies the phenomenological analysis presented in previous chapter of this report. This also indicates that the velocity

scale $Ur = S_t(\alpha_v / l_t) / \rho$ has been chosen appropriately so that the velocity of the interface motion can be calculated directly.

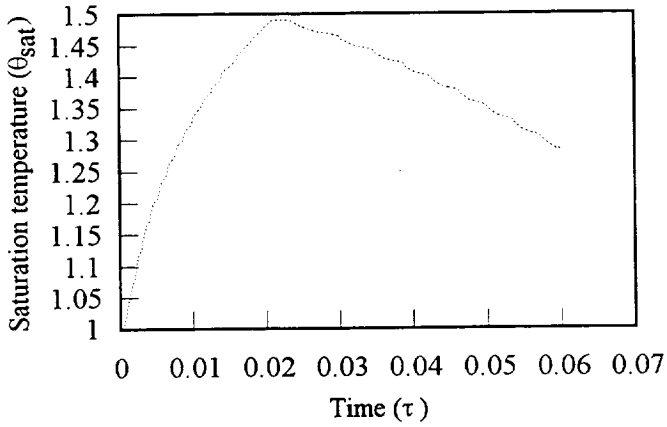

(a) Variation of saturation temperature during evaporation and condensation

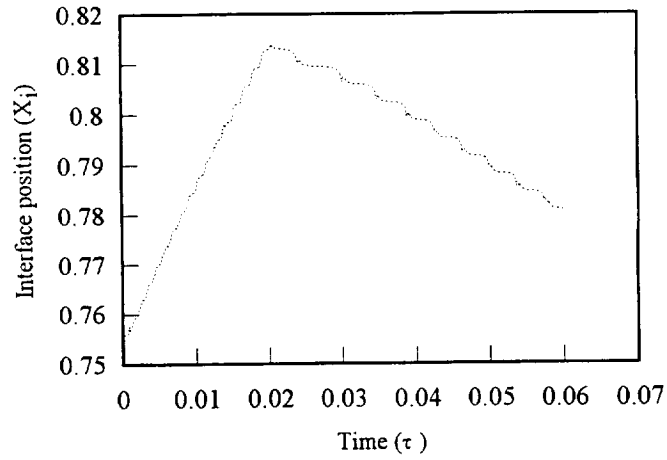

(b) Motion of interface during evaporation and condensation

Figure 5.4 Bulk evaporation and condensation

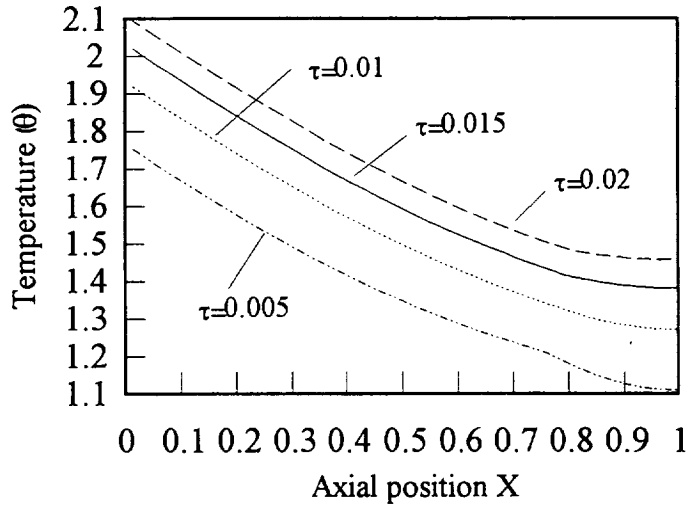

(c) Temperature distribution during evaporation

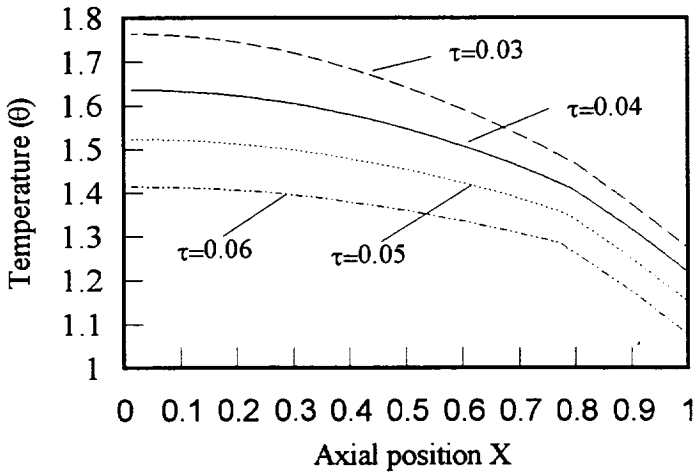

(d) Temperature distribution during condensation

Figure 5.4 (continued) Bulk evaporation and condensation

CHAPTER 6 CONCLUSIONS

In this work, a numerical method was developed to model the bulk evaporation and condensation processes in an encapsulated container. An internal energy formulation for the constant volume phase change process was successfully implemented. Some assumptions regarding the convection heat transfer rate at the vapor-liquid interface were made through scaling and order analysis. The velocity and time scales of the interface movement were obtained through scaling analysis. The dominating mechanism for the heat transfer at the interface is conduction which is modeled in the dimensionless governing equations. The convection effect induced by the density change was analyzed and found negligible.

The computational performances of the well-established enthalpy formulation and the proposed internal energy formulation were evaluated and compared. Both formulations yield identical results with similar computational efficiencies. The internal energy formulation has the advantage of having more compact form. With the internal energy formulation, the internal energy based update method was developed. The performances of two update methods for the vapor phase fraction, the E-based and T-based methods, were investigated. The E-based method is superior to the T-based method in terms of computational efficiency and formulation simplicity for evaporation and condensation problems. The E-based method is also capable of handling more complicated phase change problems, because it does not require the artificial phase change window.

The internal energy formulation and the E-based method were successfully implemented and used to compute bulk evaporation and condensation processes under different conditions. The evolution of the bulk evaporation and condensation processes was simulated. The variations of

the temperature distribution, the liquid content and the saturation temperature with time for a variety of boundary conditions were obtained. Numerical experiments and analysis verified the velocity scale of the interface motion.

This work provided a basis for further modeling of other bulk liquid-vapor phase change problems of multi-phase nuclear fuel elements, in which the buoyancy convection due to gravity effects and internal heating are involved. The modeling of thermal performace of multi-phase nuclear fuel elements under variable gravity conditions is discussed in another report.

Acknowledgments

This work was performed for the Department of Defense, Ballistic Missile Defense Organization (formerly SDIO), Innovative Science and Technology Office under contract NAS-26314, managed by NASA Lewis Research Center through INSPI.

Helpful discussions with Drs. W. Shyy and J. F. Klausner are greatly appreciated.

REFERENCES

1. J. Crank, *Free and Moving Boundary Problems,* Clarendon Press, Oxford (1984)

2. V. R Voller and C. R. Swaminathan, General source-based method for solidification phase change, *Numerical Heat Transfer, Part B*, **19**, 175-189 (1991)

3. N. Shamsundar and E. M. Sparrow, Analysis of multidimensional conduction phase change via the enthalpy model, *J. Heat Transfer*, **97**, 333-340 (1975)

4. L. S. Yao and J. Prusa, Melting and Freezing, in *Advances in Heat Transfer*, Hartnett et al. ed., Academic Press, Inc., San Diego, **19**, 23-85 (1989)

5. A. A. Samarskii, P. N. Vabishchevich, O. P. Iliev and A. G. Churbanov, Numerical simulation of convection/diffusion phase change problems-A Review, *Int. J. Heat Mass Transfer*, **36**, 4095-4106 (1993)

6. C. Prakash, M. Samonds and A. K. Singhal, A fixed grid numerical modeling methodology for phase change problems involving a moving heat source, *Int. J. Heat Mass Transfer*, **30**, 2690-94 (1987)

7. W. Shyy and M.-H. Chen, Interaction of thermocapillary and natural convection flows during solidification: normal and reduced gravity conditions, *J. Crystal Growth*, **108**, 247-261 (1991)

8. W. Shyy, Y. Pang, G. B. Hunter, D. Y. Wei and M.-H Chen, Modeling of turbulent transport and solidification during continuous ingot casting, *Int. J. Heat Mass Transfer*, **35**, 1229-1245 (1992)

9. W. Shyy, H. S. Udaykumar S.-J. and Liang, An interface tracking method applied to morphological evolution during phase change, *Int. J. Heat Mass Transfer*, **36**, 1833-1844 (1993)

10. W. Shyy and M. M. Rao, Enthalpy based formulations for phase-change problems with application to g-jitters, *Microgravity Sci. Technology*, 7, 41-49 (1994)

11. W. Shyy, *Computational Modeling for Fluid Flow and Interfacial Transport*, Elsevier, Amsterdam, The Netherlands (1994)

12. W. Shyy, S.-J. Liang and Y. W. Daniel, Effect of dynamic perturbation and contact condition on edge-defined fiber growth characteristics, *Int. J. Heat Mass Transfer*, **37**, 977-987 (1994)

13. C. K Hsieh and C.-Y. Choi, Solution of one- and two-phase melting and solidification problems imposed with constant or time-variant temperature and flux boundary conditions, *J. Heat Transfer*, **114**, 524-528 (1992)

14. C. K. Hsieh, M. Akbari and H. Li, Solution of inverse Stefan problems by a source-and-sink method, *Int. J. Numerical Methods for Heat and fluid Flow*, **2**, 391-406 (1993)

15. W. P. Jones and U. Renz, Condensation from a turbulent stream onto a vertical surface, *Int. J. Heat Mass Transfer*, **17**, 1019-1028 (1974)

16. R. Cossmann, H.-P. Odenthal and U. Renz, Heat and mass transfer during partial condensation in a turbulent pipe flow, *Proc. 7th Int. Heat Transfer Conf.*, U. Grigul et al. ed., Hemisphere Publishing Corp., Washington, D.C. (1982)

17. M. Gaultier, M. Lezaun and F. Vadillo, A Problem of heat and mass transfer: proof of the existence condition by a finite difference method, *Int. J. numerical Methods in Fluids*, **16**, 87-104 (1993)

18. J.-M. Tournier and M. S. El-Genk, "HPTAM" Heat-pipe transient analysis model: an analysis of water heat pipes, *Proc. 9th Symp. Space Nuclear Power Systems*, Conf-920104 (1992)

19. J. H. Jang, A. Faghri, W. S. Chang and E. T. Mahefkey, Mathematical modeling and analysis of heat pipe start-up from the frozen state, *J. Heat Transfer*, **112**, 586-594 (1990)

20. W. Shyy, W. K. Gringrich, W. J. Krotiuk and J. E. Fredley, Transient two-phase heat transfer in a capillary-pumped-loop reservoir for spacecraft thermal management, *Proc. 10th Symp.m on Space Nuclear Power and Propulsion*, Conf-930103, American Institute of Physics (1993)

21. W. C. Reynolds, *Thermodynamic Properties in SI*, Dept. of Mechanical Engineering, Stanford University (1979)

22. Z. Ding and S. Anghaie, Numerical investigation of the two-phase equilibrium state in a cylindrical nuclear fuel cell under zero gravity condition, *6th AIAA/ASME Joint Thermophysics and Heat Transfer Conf.*, Colorado Springs, CO, AIAA 94-1995 (1994)

23. Z. Ding and S. Anghaie, Modeling of R-12 bulk evaporation in an encapsulated container, *ASME Intl. Mechanical Engineering Congress & Exhibition*, Chicago, IL, (1994)

24. M. N. Ozisik, *Heat Conduction*, John Wiley, New York (1980)

REPORT DOCUMENTATION PAGE

Form Approved
OMB No. 0704-0188

1. AGENCY USE ONLY (*Leave blank*)	2. REPORT DATE	3. REPORT TYPE AND DATES COVERED
	April 1996	Final Contractor Report

4. TITLE AND SUBTITLE

Modeling of Bulk Evaporation and Condensation

5. FUNDING NUMBERS

WU-233-01-0N
C-NAS3-26314

6. AUTHOR(S)

S. Anghaie and Z. Ding

7. PERFORMING ORGANIZATION NAME(S) AND ADDRESS(ES)

University of Florida
Ultrahigh High Temperature Reactor and Energy Conversion Program
Innovative Nuclear Space Power and Propulsion Institute
Gainesville, Florida 32611

8. PERFORMING ORGANIZATION REPORT NUMBER

E-9885

9. SPONSORING/MONITORING AGENCY NAME(S) AND ADDRESS(ES)

National Aeronautics and Space Administration
Lewis Research Center
Cleveland, Ohio 44135-3191

10. SPONSORING/MONITORING AGENCY REPORT NUMBER

NASA CR-198392

11. SUPPLEMENTARY NOTES

Project Manager, Harvey S. Bloomfield, Power Technology Division, NASA Lewis Research Center, organization code 5440, (216) 433-6131.

12a. DISTRIBUTION/AVAILABILITY STATEMENT

Unclassified - Unlimited
Subject Categories 34 and 66

This publication is available from the NASA Center for Aerospace Information, (301) 621-0390.

12b. DISTRIBUTION CODE

13. ABSTRACT (*Maximum 200 words*)

This report describes the modeling and mathematical formulation of the bulk evaporation and condensation involved in liquid-vapor phase change processes. An internal energy formulation, for these phase change processes that occur under the constraint of constant volume, was studied. Compared to the enthalpy formulation, the internal energy formulation has a more concise and compact form. The velocity and time scales of the interface movement were obtained through scaling analysis and verified by performing detailed numerical experiments. The convection effect induced by the density change was analyzed and found to be negligible compared to the conduction effect. Two iterative methods for updating the value of the vapor phase fraction, the energy based (E-based) and temperature based (T-based) methods, were investigated. Numerical experiments revealed that for the evaporation and condensation problems the E-based method is superior to the T-based method in terms of computational efficiency. The internal energy formulation and the E-based method were used to compute the bulk evaporation and condensation processes under different conditions. The evolution of the phase change processes was investigated. This work provided a basis for the modeling of thermal performance of multi-phase nuclear fuel elements under variable gravity conditions, in which the buoyancy convection due to gravity effects and internal heating are involved.

14. SUBJECT TERMS	15. NUMBER OF PAGES
Liquid-vapor phase change; Mathematical model; Constant volume process	38
	16. PRICE CODE: A03

17. SECURITY CLASSIFICATION OF REPORT	18. SECURITY CLASSIFICATION OF THIS PAGE	19. SECURITY CLASSIFICATION OF ABSTRACT	20. LIMITATION OF ABSTRACT
Unclassified	Unclassified	Unclassified	